Journal of
Medicinal
Chemistry

Volume 48, Number 22 November 3, 2005

Letters

Design and Synthesis of Peptidomimetic Severe Acute Respiratory Syndrome Chymotrypsin-like Protease Inhibitors

Arun K. Ghosh,*,§,† Kai Xi,§,† Kiira Ratia,⊥ Bernard D. Santarsiero,⊥ Wentao Fu,⊥ Brian H. Harcourt,¶ Paul A. Rota,¶ Susan C. Baker,# Michael E. Johnson,⊥ and Andrew D. Mesecar⊥

Departments of Chemistry and Medicinal Chemistry, Purdue University, West Lafayette, Indiana 47907, Department of Chemistry, University of Illinois at Chicago, Chicago, Illinois 60607, Center for Pharmaceutical Biotechnology and Department of Medicinal Chemistry and Pharmacognosy, University of Illinois at Chicago, 900 S. Ashland, Illinois 60607, Department of Microbiology and Immunology, Loyola University of Chicago, Stritch School of Medicine, Maywood, Illinois, and Center for Disease Control and Prevention, Atlanta, Georgia

Received June 10, 2005

Abstract: Design, synthesis, and biological evaluation of peptidomimetic severe acute respiratory syndrome chymotrypsin-like protease (SARS-3CLpro) inhibitors for severe acute respiratory syndrome coronavirus (SARS-CoV) are described. These inhibitors exhibited antiviral activity against SARS-CoV in infected cells in the micromolar range. An X-ray crystal structure of our lead inhibitor (**4**) bound to SARS-3CLpro provided important drug-design templates for the design of small-molecule inhibitors.

Severe acute respiratory syndrome (SARS) is an acute respiratory illness caused by a novel human coronavirus, SARS-CoV.[1] Since its first report in Guangdong Province, China, in November 2002, SARS has spread to other Asian countries, North America, and Europe.[1,2] This epidemic affected more than 8000 reported individuals by July 2003 and resulted in 774 deaths. Thus far, no effective therapy exists for this virus. During viral replication, the RNA-dependent RNA polymerase is extensively processed by two viral proteases, chymotrypsin-like protease (3CLpro) and papain-like protease (PLpro).[3] As a consequence, these proteases are recognized as attractive targets for drug development for SARS and related infections.[4]

The structure and activity of the coronavirus 3CLpro has already been eludicated.[5] It contains a catalytic dyad in the active site where a cysteine residue acts as a nucleophile and a histidine residue acts as the general acid base. The design of inhibitors of 3CLpro as therapeutics was particularly interesting because 3CLpro is functionally analogous to the main picornaviral protease 3Cpro and significant drug-design efforts for human rhinoviral 3Cpro are already well precedented.[6] These studies have provided important molecular insights that may aid the design of novel inhibitors of SARS-3CLpro. Herein, we report our preliminary investigation that led to the design and synthesis of peptidomimetic inhibitors of SARS-3CLpro inhibitors. The inhibitors have been shown to block the replication of SARS-CoV in cell culture assay. Furthermore, we have determined the X-ray structure of an inhibitor complexed with SARS-3Clpro at a resolution of 1.9 Å.

Our initial design of SARS-3CLpro inhibitors was based on examination of the superimposed X-ray crystal structure of the related enzyme of porcine transmissible gastroenteritis (corona)virus (TGEV M^{Pro}) and a substrate-analogue hexapeptidyl chloromethyl ketone (CMK) inhibitor (**1**) and from structural information derived from modeled lead inhibitor AG-7088 (**2**) in the 3CL-pro active site (Figure 1).[5,7] Inhibitor **2** is ineffective against SARS-CoV in cell culture assay. Antiviral activity for **2** was reported to be >100 μg/mL.[8] It appeared that the vinylogous group of the ethyl ester of **2** may interact with residues similar to the chloromethyl ketone functionality of inhibitor **1**. Both inhibitors bind to their respective targets through covalent bonding with the active site cysteine residue. The S2-subsites

* To whom correspondence should be addressed. Phone: 765-494-5323. Fax: 765-496-1612. E-mail: akghosh@purdue.edu.
§ Purdue University.
† Department of Chemistry, University of Illinois at Chicago.
⊥ Center for Pharmaceutical Biotechnology and Department of Medicinal Chemistry and Pharmacognosy, University of Illinois at Chicago.
¶ Center for Disease Control and Prevention.
# Loyola University of Chicago.

10.1021/jm050548m CCC: $30.25
Published on Web 10/04/2005

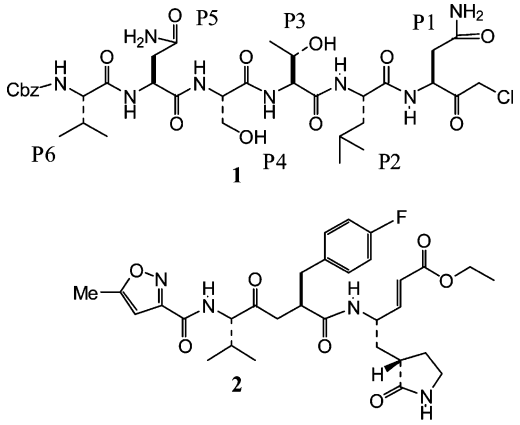

Figure 1. Structures of inhibitors **1** and **2**.

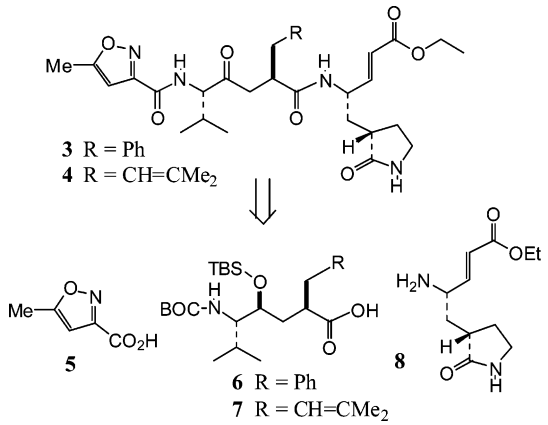

Figure 2. Key fragments for inhibitors **3** and **4**.

Scheme 1

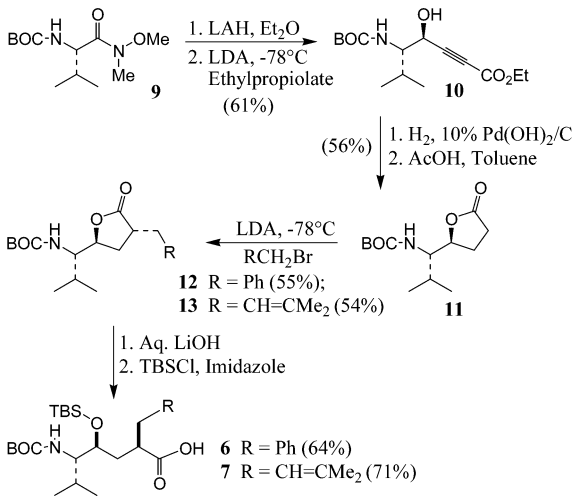

Scheme 2

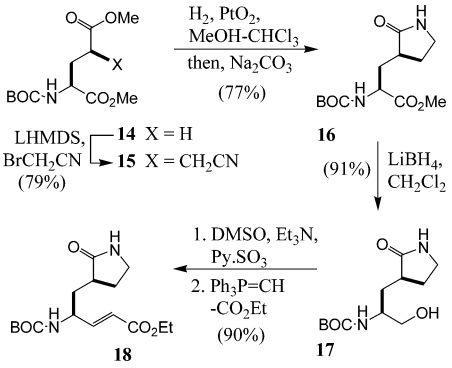

of both enzymes are quite different. The P2-residue of inhibitor **1** is Leu, and the corresponding P2 side chain for inhibitor **2** is a *p*-fluorophenylmethyl group. Therefore, it appears that the P2-*p*-fluorophenylmethyl group in **2** is too large for the S2-pocket.[5a] Our preliminary modeling studies indicate that a P2-phenylmethyl or other designed side chains may result in potent inhibitors for SARS-3CLpro. Since the autocleavage site of SARS-CoV contains a P2-Phe, incorporation of the P2-benzyl side chain may be accommodated as well.[6] On the basis of this rationale, we have prepared and evaluated inhibitors containing phenylmethyl and prenyl side chains as the P2-ligand (Figure 2). These inhibitors possess a P1/P1′-Michael acceptor α,β-unsaturated ester functionality, which is expected to link to the Cys-145 covalently. In addition to varying the P2-side chains, we have also investigated a hydroxyethylene isostere in place of the ketoethylene isostere. Since covalent bound inhibitors often exhibit toxicity, our ultimate goal is to design noncovalent and reversible SARS-3CLpro inhibitors.

The 3CLpro inhibitors depicted in Figure 2 were synthesized by assembly of key fragments isoxazole carboxylic acid **5**, dipeptide isostere (**6** and **7**), and γ-lactam derivative **8**. The synthesis of dipeptide isosteres for inhibitors **3** and **4** is outlined in Scheme 1. Commercial Boc-L-valine was converted to Weinreb amide **9** by treatment with isobutyl chloroformate and 1-methylpiperidine followed by treatment of the resulting mixed anhydride with *N*,*O*-dimethylhydroxylamine. Reduction of **9** with lithium aluminum hydride in diethyl ether provided the aldehyde, which was reacted with lithium propiolate derived from the treatment of ethyl propiolate and lithium diisopropylamide to furnish the acetylenic alcohol **10** as an inseparable mixture (3.4:1) of diastereomers. Catalytic hydrogenation of **10** followed by acid-catalyzed lactonization of the resulting γ-hydroxy ester with a catalytic amount of acetic acid in toluene at reflux afforded γ-lactone **11** in 56% yield after silica gel chromatography. For introduction of the desired alkyl group at C-2, lactone **11** was treated with lithium diisopropylamide (2.2 equiv) in THF at −78 °C (30 min). The resulting enolate was reacted with benzyl bromide (1.1 equiv) or 4-bromo-2-methyl-2-butene (1.1 equiv) for 30 min at −78 °C to provide the respective alkylated lactone **12** or **13**.[9] Lithium hydroxide promoted hydrolysis of lactones **12** and **13** followed by protection of the resulting γ-hydroxyl group with *tert*-butyldimethylsilyl chloride in the presence of imidazole in DMF provided the carboxylic acids **6** and **7** in 64% and 71% yields, respectively.

The synthesis of P2-lactam ligand **8** is outlined in Scheme 2. Optically pure glutamic acid was converted into *N*-Boc-L-(+)-glutamic acid dimethyl ester **14** as described previously.[10] Diester **14** was converted into alkylated product **15** by utilizing 1,3-asymmetric induction by the dianionic alkylation protocol developed by Hanessian.[11] Thus, treatment of **14** with LHMDS (2.2 equiv) at −78 °C provided the enolate, which was alkylated with bromoacetonitrile (1.1 equiv) to give alkylated product **15** as a single diastereomer. The rationale for similar diastereoselectivity was previously

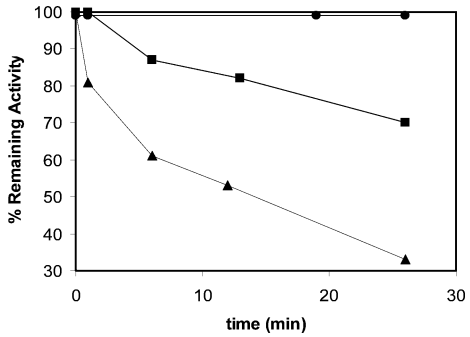

Figure 3. Time course of inactivation of SARS 3CLpro by **3** (■) and **4** (▲) versus a DMSO control (●).

reported by Hanessian.[11] The nitrile derivative **15** was subjected to hydrogenation in the presence of PtO_2 and chloroform.[12] The resulting amine salt was treated with Na_2CO_3 at reflux for 6 h to afford lactam ester **16**.[13]

Selective reduction of the ester group in the presence of the lactam was carried out with $LiBH_4$ (1 N solution in THF) in CH_2Cl_2 to provide alcohol **17** in 91% yield. Alcohol **17** was converted into desired lactam fragment **18** by a one-pot oxidation followed by Wittig reaction of the resulting aldehyde with carbethoxyphosphorane in DMSO in 90% yield.

The synthesis of inhibitors **3** and **4** is outlined in Scheme 3. Exposure of **18** to trifluoroacetic acid (20% in CH_2Cl_2) effected the removal of the Boc group. To the resulting TFA salt, Hunig's base was added to liberate the free amine. It was coupled with acids **6** and **7** to provide amide derivatives **19** and **20**, respectively. Treatment of these amides with trifluoroacetic acid in dichloromethane afforded the corresponding amine, which was coupled with known 5-methylisoxazole-3-carboxylic acid **5**[14] to furnish silyl derivatives **21** and **22**. Removal of silyl group with 48% aqueous hydrofluoride acid in tetrahydrofuran and oxidation of the resulting alcohol with Dess−Martin periodinane furnished inhibitors **3** and **4**. Inhibitor **23** with a hydroxyethylene isostere was prepared by deprotection of the silyl group from **21**.

The above synthetic inhibitors were evaluated in a FRET-based microplate assay developed to measure the activity of SARS-3CLpro.[15] The inactivation rate constant k_{inact} and half-life $T_{1/2}$ of SARS-3CLpro in the presence of these compounds and in the presence of E64,[16] a standard cysteine protease inhibitor, have been quantitated. The time course for inactivation of SARS-CoV 3CLpro is shown in Figure 3 for each of these compounds, and the k_{inact} and $T_{1/2}$ values resulting from a fit of the data to a single-exponential equation are summarized in Table 1. The data indicate that **4** is the best inhibitor with a $T_{1/2}$ of ~15 min. Compound **23**, with a hydroxyethylene isostere, and E64 did not inhibit the enzyme under the conditions assayed.

Scheme 3

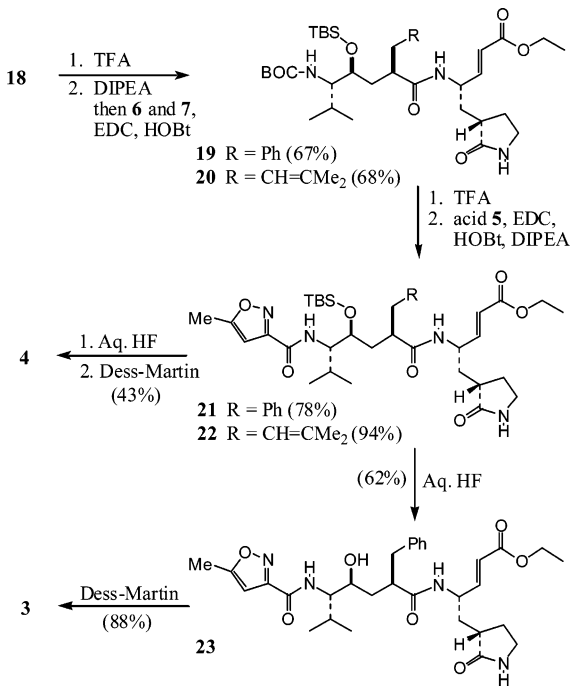

Table 1. Inactivation Rate Constants for SARS-CoV 3CLpro by Compounds

inhibitor	k_{inact} (min^{-1})	3CLpro $T_{1/2}$ (min)
E64	0.0022 ± 0.0013	315 ± 302
3	0.014 ± 0.0017	49 ± 6
4	0.045 ± 0.0095	15 ± 3
23	0.0025 ± 0.00038	277 ± 43

The antiviral activity of synthetic inhibitors was also evaluated in a neutral red assay developed on the basis of the work of Huggins and co-workers.[17] The antiviral IC_{50} of **3** and **4** were shown to be approximately 45 and 70 μM, respectively.

No toxicity is observed up to the maximum concentration of compound tested, which was 100 μM. Significant antiviral activity of E64d was not observed up to 100

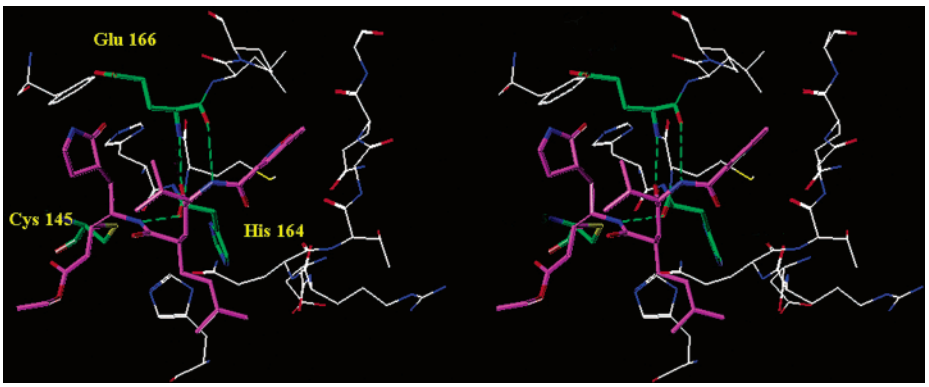

Figure 4. X-ray crystal structure of **4** (thick stick with magenta carbon) with SARS 3CLpro. Hydrogen bonds between inhibitor and $3Cl^{pro}$ are shown as green dotted lines.

μM, but observable toxicity was noted. Since inhibitor **4** with a P2-prenyl group is significantly more potent than the P2-phenylmethyl containing inhibitor **3** in vitro, it indicates that other side chain residues could be accommodated by the S2-subsite of 3CLpro.

To gain molecular insight, we attempted to resolve the inhibitor-bound crystal structure of SARS-3CLpro. We successfully crystallized the nontagged SARS-3CLpro apoenzyme in complex, i.e., covalently modified, with inhibitor **4**. The X-ray structure of SARS-3CLpro inhibitor complex of **4** was determined to a resolution of 1.89 Å.[18] A stereoview of the inhibitor-bound structure is shown in Figure 4. Analysis of this structure reveals why **23** shows very little inhibitory activity of the enzyme. It indicates that substitution of the carbonyl oxygen atom with a hydroxyl group disrupts an important hydrogen bond between the backbone amide nitrogen of Glu166 and the carbonyl oxygen of the inhibitor. This SARS-3CLpro-bound inhibitor structure will provide molecular insight and facilitate design of more effective inhibitors.

In conclusion, our preliminary investigation led to identification of two peptidomimetic lead inhibitors for SARS-3CLpro. These inhibitors are not only potent against SARS-3CLpro but effective in SARS-CoV cell culture assay. An inhibitor containing a hydroxyethylene isostere scaffold was not very effective. An X-ray structure of **4**-bound SARS-3CLpro revealed important molecular insights into the molecular recognition of this class of compounds by SARS-3CLpro. Further investigations including detailed structure−activity relationships and nonpeptidal inhibitor design from these preliminary studies are currently underway.

Acknowledgment. This work was supported by the National Institutes of Health (NIAID), Grant P01 AI060915. The work was also partially supported by NIGMS (Grant GM 53386).

Supporting Information Available: Experimental methods for **3**−**23** and HPLC data for **3**, **4**, and **23**. This material is available free of charge via the Internet at http://pubs.acs.org.

References

(1) (a) Drosten, C.; Gunther, S.; Preiser, W.; van der Werf, S.; Brodt, H. R.; Becker, S.; Rabenau, H.; Panning, M.; Kolesnikova, L.; Fouchier, R. A.; Berger, A.; Burguiere, A. M.; Cinatl, J.; Eickmann, M.; Escriou, N.; Grywna, K.; Kramme, S.; Manuguerra, J. C.; Muller, S.; Rickerts, V.; Sturmer, M.; Vieth, S.; Klenk, H. D.; Osterhaus, A. D.; Schmitz, H.; Doerr, H. W. Identification of a novel coronavirus in patients with severe acute respiratory syndrome. *N. Engl. J. Med.* **2003**, *348*, 1967−1976. (b) Ksiazek, T. G.; Erdman, D.; Goldsmith, C. S.; Zaki, S. R.; Peret, T.; Emery, S.; Tong, S.; Urbani, C.; Comer, J. A.; Lim, W.; Rollin, P. E.; Dowell, S. F.; Ling, A. E.; Humphrey, C. D.; Shieh, W. J.; Guarner, J.; Paddock, C. D.; Rota, P.; Fields, B.; DeRisi, J.; Yang, J. Y.; Cox, N.; Hughes, J. M.; LeDuc, J. W.; Bellini, W. J.; Anderson, L. J. A novel coronavirus associated with severe acute respiratory syndrome. *N. Engl. J. Med.* **2003**, *348*, 1953−1966.

(2) Peiris, J. S.; Lai, S. T.; Poon, L. L.; Guan, Y.; Yam, L. Y.; Lim, W.; Nicholls, J.; Yee, W. K.; Yan, W. W.; Cheung, M. T.; Cheng, V. C.; Chan, K. H.; Tsang, D. N.; Yung, R. W.; Ng, T. K.; Yuen, K. Y. Coronavirus as a possible cause of severe acute respiratory syndrome. *Lancet* **2003**, *361*, 1319−1325 and references therein.

(3) Rota, P. A.; Oberste, M. S.; Monroe, S. S.; Nix, W. A.; Campagnoli, R.; Icenogle, J. P.; Penaranda, S.; Bankamp, B.; Maher, K.; Chen, M. H.; Tong, S.; Tamin, A.; Lowe, L.; Frace, M.; DeRisi, J. L.; Chen, Q.; Wang, D.; Erdman, D. D.; Peret, T. C.; Burns, C.; Ksiazek, T. G.; Rollin, P. E.; Sanchez, A.; Liffick, S.; Holloway, B.; Limor, J.; McCaustland, K.; Olsen-Rasmussen, M.; Fouchier, R.; Gunther, S.; Osterhaus, A. D.; Drosten, C.; Pallansch, M. A.; Anderson, L. J.; Bellini, W. J. Characterization of a novel coronavirus associated with severe acute respiratory syndrome. *Science* **2003**, *300*, 1394−1399.

(4) Thiel, V.; Ivanov, K. A.; Putics, A.; Hertzig, T.; Schelle, B.; Bayer, S.; Weissbrich, B.; Snijder, E. J.; Rabenau, H.; Doerr, H. W.; Gorbalenya, A. E.; Ziebuhr, J. Mechanisms and enzymes involved in SARS coronavirus genome expression. *J. Gen. Virol.* **2003**, *84*, 2305−2315.

(5) (a) Anand, K.; Ziebuhr, J.; Wadhwani, P.; Mesters, J. R.; Hilgenfeld, R. Coronavirus main proteinase (3CL(pro)) structure: Basis for design of anti-SARS drugs. *Science* **2003**, *300*, 1763−1767. (b) Anand, K.; Palm, G. J.; Mesters, J. R.; Siddell, S. G.; Ziebuhr, J.; Hilgenfeld, R. Structure of coronavirus main proteinase reveals combination of a chymotrypsin fold with an extra alpha-helical domain. *EMBO J.* **2002**, *21*, 3213−3224.

(6) Hegyi, A.; Ziebuhr, J. Conservation of substrate specificities among coronavirus main proteases. *J. Gen. Virol.* **2002**, *83*, 595−599.

(7) Matthews, D. A.; Dragovich, P. S.; Webber, S. E.; Fuhrman, S. A.; Patick, A. K.; Zalman, L. S.; Hendrickson, T. F.; Love, R. A.; Prins, T. J.; Marakovits, J. T.; Zhou, R.; Tikhe, J.; Ford, C. E.; Meador, J. W.; Ferre, R. A.; Brown, E. L.; Binford, S. L.; Brothers, M. A.; DeLisle, D. M.; Worland, S. T. Structure-assisted design of mechanism-based irreversible inhibitors of human rhinovirus 3C protease with potent antiviral activity against multiple rhinovirus serotypes. *Proc. Natl. Acad. Sci. U.S.A.* **1999**, *96*, 11000−11007.

(8) Matthews, D. A.; Patick, A. K.; Baker, R. O.; Brothers, M. A.; Dragovich, P. S.; Hartmann, C. J.; Johnson, T. O.; Mucker, E. M.; Reich, S. H.; Rejto, P. A. J.; Rose, P. W.; Zwiers, S. H.; Huggins, J. W. *In Vitro Antiviral Activity of Human Rhinovirus 3C Protease Inhibitors against the SARS Coronavirus*; The National Academies Press: Washington, DC, 2004; Chapter 4, pp 186−193 (http://www.nap.edu/books/0309091543/html/186.html).

(9) Ghosh, A. K.; Fidanze, S. Transition-state mimetics for HIV protease inhibitors: Stereocontrolled synthesis of hydroxyethylene and hydroxyethylamine isosteres by ester-derived titanium enolate syn and anti-aldol reactions. *J. Org. Chem.* **1998**, *63*, 6146−6154.

(10) Kokotos, G.; Padron, J. M.; Martin, T.; Gibbons, W. A.; Martin, V. S. A general approach to the asymmetric synthesis of unsaturated lipidic α-amino acids. The first synthesis of α-aminoarachidonic acid. *J. Org. Chem.* **1998**, *63*, 3741−3744.

(11) Hanessian, S.; Margarita, R. 1,3-Asymmetric induction in dianionic allylation reactions of amino acid derivatives. Synthesis of functionally useful enantiopure glutamates, pipecolates, and pyroglutamates. *Tetrahedron Lett.* **1998**, *39*, 5887−5890.

(12) Secrist, J. A., III; Logue, M. W. Amine hydrochlorides in the reduction in the presence of chloroform. *J. Org. Chem.* **1972**, *37*, 335−336.

(13) Tian, Q.; Nayyar, N. K.; Babu, S.; Chen, L.; Tao, J.; Lee S.; Tibbetts, A.; Moran, T.; Liou, J.; Guo, M.; Kennedy, T. P. An efficient synthesis of a key intermediate for the preparation of the rhinovirus protease inhibitor AG7088 via asymmetric dianionic cyanomethylation of *N*-Boc-L-(+)-glutamic acid dimethyl ester. *Tetrahedron Lett.* **2001**, *42*, 6807−609.

(14) Baraldi, P. G.; Simoni, D.; Moroder, F.; Manfredini, S.; Mucchi, L.; Vecchia, F. D. Synthesis of 2-(5′-substituted isoxazol-3′-yl)-4-oxo-3-thiazolidinyl alkanoic acids. *J. Heterocycl. Chem.* **1982**, *19*, 557−560.

(15) Enzymatic activity of recombinant SARS-3CLpro was measured via a FRET-based fluorescence assay using the peptide-substrate E(EDANS)-S-A-T-L-Q-S-G-L-A-K(DABCYL)-S (SynPep, Inc.). The reactions were monitored at 25 °C in 96-well microplates containing 50 mM HEPES (pH 7.5) using a Varian Eclipse spectrofluorimeter. For time course of inactivation studies, 50 μM 3CLpro was incubated with 500 μM of each compound. The percent remaining activity as a function of time was plotted, and the data were fit to a single-exponential decay to obtain k_{inact} and half-life T. Details of this assay will be published in due course.

(16) Kim, J. C.; Spence, R. A.; Currier, P. F.; Lu, X.; Denison, M. R. Coronavirus protein processing and RNA synthesis is inhibited by the cysteine proteinase inhibitor E64d. *Virology* **1995**, *208*, 1−8.

(17) Baker, R. O.; Bray, M.; Higgins, J. W. Potential antiviral therapeutics for smallpox, monkeypox and orthopoxvirus infections. *Antiviral Res.* **2003**, *57*, 13−20.

(18) The protein−ligand X-ray structure of **4**-bound SARS-3 CLpro has been deposited in PDB. RCSB code is RCSB034045 and PDB code is 2ALV. SARS-3CLpro (40−40 mg/mL) was incubated with a 2-fold molar excess of **4** for 3 h. The enzyme−inhibitor complex was then crystallized at pH 7.5 using PEG 20,000. Crystals were soaked in the mother liquor plus 15% (v/v) MPD and then flash-frozen using a nitrogen-gas stream. Diffraction data on a single crystal were recorded on an MAR 210 CCD detector at SER-CAT beamline 22-ID. Data were integrated and scaled using DENZO and SCALEPACK, resulting in an R_{merge} of 3.8% for all data from 50 to 1.9 Å. The 3CLpro−**4** complex crystallized in space group $C121$ with one molecule in the asymmetric unit with

unit cell parameters of $a = 107.1$ Å, $b = 83.2$ Å, $c = 53.7$ Å, and $\beta = 104.4°$. The structure was determined by molecular replacement using PDB code 1M4H as a search model. The structure was built and refined using the programs O and CNS. The final R_{cryst} and R_{free} values were 25.9% and 28.4%, respectively. The final model includes the inhibitor covalently linked to Cys145.

JM050548M